ACES Asian Chemical Editorial Society

doi.org/10.1002/ajoc.202500521

ASIAN JOURNAL OF ORGANIC CHEMISTRY
Research Article

www.asianjoc.org

Cyclotetrabenzil Oxime Derivatives

Thusini P. Hemachandra,[a] Bhawna Kumari,[b] Yun-Hsien Lin,[b] Ashikur Rabbi,[a] Thamon Puangsamlee,[a] Xiqu Wang,[a] Soumya Mukherjee,*[b] and Ognjen Š. Miljanić*[a, c]

Dedicated to the memory of Prof. Masahiko Iyoda, whose marvelous molecules continue to inspire us.

Cyclotetrabenzil, a shape-persistent macrocyclic octaketone, is found to undergo eightfold condensation with hydroxylamine hydrochloride to yield its octaoxime. Subsequent acetylation of this macrocyclic oxime afforded the corresponding octaoxime acetate. Single-crystal X-ray diffraction reveals that both new derivatives assemble into nanotubular structures. However, their packing differs: the oxime forms hydrogen-bonded tubes that bundle via included dimethyl sulfoxide (DMSO) molecules, whereas the acetate—lacking hydrogen-bond donors—forms more loosely packed tubes with molecules tilted ~54.5° relative to the tube axis. Gas sorption studies (CO_2, C_2, and C_3 hydrocarbons) show that cyclotetrabenzil is nonporous, whereas the oxime and acetate exhibit modest microporosity with BET surface areas of ~200 $m^2\ g^{-1}$. Both derivatives display preferential uptake of propyne over propene and propane, and the acetate also adsorbs more acetylene than ethylene or ethane. Nonetheless, these capacities and selectivities are suboptimal for dynamic separation of C_2 and C_3 hydrocarbons. This study illustrates how oxime functionalization can modulate macrocyclic assembly and gas uptake behavior, providing insights for the design of future porous organic macrocycles.

1. Introduction

Cyclobenzoins[1,2] are mostly shape-persistent macrocycles which are readily prepared by a benzoin condensation of aromatic dialdehydes. Oxidation of the parent cyclotetrabenzoin[3] produces cyclotetrabenzil octaketone, which has been used as a component of lithium-ion[4] and aluminum[5] batteries, and a precursor to porous organic polymers[6–8] and optoelectronic materials.[9] Stimulated by the interest in this class of macrocycles, we decided to explore the effects of their modification into oximes. Oximes have recently been used in the preparation of conductive metal-organic frameworks,[10] in detoxification of organophosphate reagents,[11,12] as materials for the removal of uranium from seawater,[13–15] and as building blocks for dynamic chemical networks.[16] In this contribution, we report the synthesis of cyclotetrabenzil oxime and its acetate, their crystal structures, and the investigation of their gas sorption behavior.

[a] T. P. Hemachandra, A. Rabbi, T. Puangsamlee, X. Wang, O. Š. Miljanić
Department of Chemistry, University of Houston, 3585 Cullen Boulevard #112, Houston, TX 77204-5003, USA
E-mail: miljanic@uh.edu

[b] B. Kumari, Y.-H. Lin, S. Mukherjee
Department of Chemical Sciences, Bernal Institute and Research Ireland Centre for Pharmaceuticals (SSPC), University of Limerick, Limerick V94 T9PX, Ireland
E-mail: Soumya.Mukherjee@ul.ie

[c] O. Š. Miljanić
Faculty of Chemical Engineering, Industrial University of Ho Chi Minh City, Ho Chi Minh City 71408, Vietnam

Supporting information for this article is available on the WWW under https://doi.org/10.1002/ajoc.202500521

2. Results and Discussion

Cyclotetrabenzil oxime (**2**, Scheme 1) was prepared in 49% yield by an eightfold condensation of cyclotetrabenzil (**1**)[17–19] with hydroxylamine hydrochloride. Subsequent acetylation of **2** with Ac_2O produced cyclotetrabenzil oxime acetate (**3**) in 64% yield. The two compounds were purified by recrystallization from H_2O. Both compounds are white powders, and their spectral information is consistent with the structures in Scheme 1; their simple ^1H NMR spectra suggest free rotation of the phenylene rings around their C1–C4 axes at room temperature. With **2** in hand, we were intrigued by the possibility of an eightfold Beckmann rearrangement of this material; unfortunately, extensive experimentation yielded no evidence of rearrangement and only starting material could be recovered. Thermogravimetric analyses (TGA) of **1**–**3** (Figure S7) indicate the onset of decomposition of **2** and **3** at about 60 °C lower temperature than that of octaketone **1**; tentatively, this difference can be attributed to the cleavage of the relatively weak N—O bonds.

Single crystals of oxime **2** were grown over 2 days by vapor diffusion of dichloromethane into a 3 mM solution of **2** in a 60:4:5 mixture of acetone, dimethyl sulfoxide (DMSO), and H_2O.[20] Oxime **2** crystallizes in *P*2/c space group with two molecules in the unit cell, along with two molecules of the DMSO solvent per molecule of **2**; one of these solvent molecules is disordered. The central macrocycle adopts a roughly square-shaped conformation (Figure 1A), with the planes of the phenylene rings on the opposite sides of the macrocycle describing angles of 40.1 and 41.7°. The ═N—OH groups on the neighboring carbon atoms are pointing in the opposite directions, and the overall molecule adopts the ···up-down-Ph-down-up-Ph-up-down-Ph-down-up··· conformation of its oxime moieties. No intramolecular hydrogen

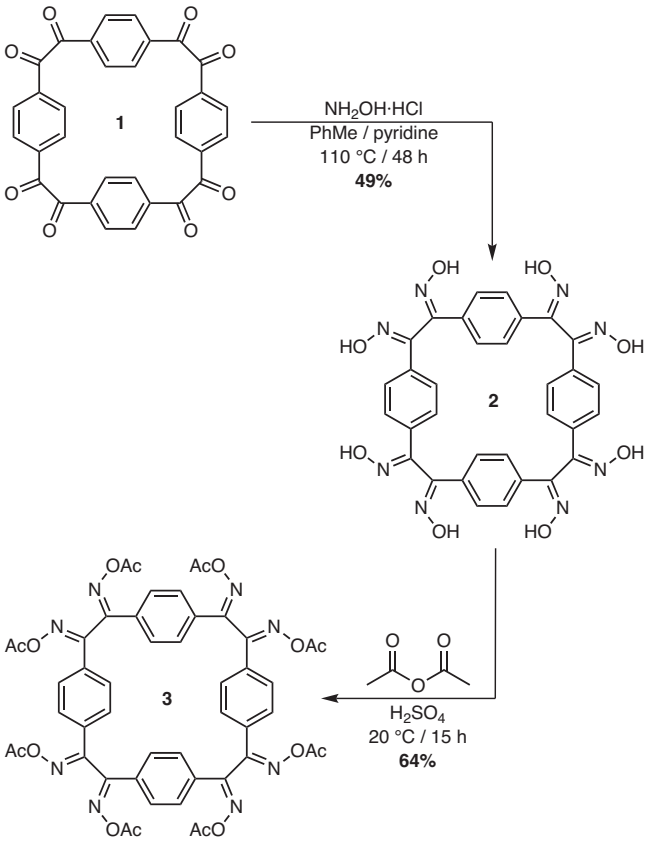

Scheme 1. Synthesis of cyclotetrabenzil oxime derivatives **2** and **3**.

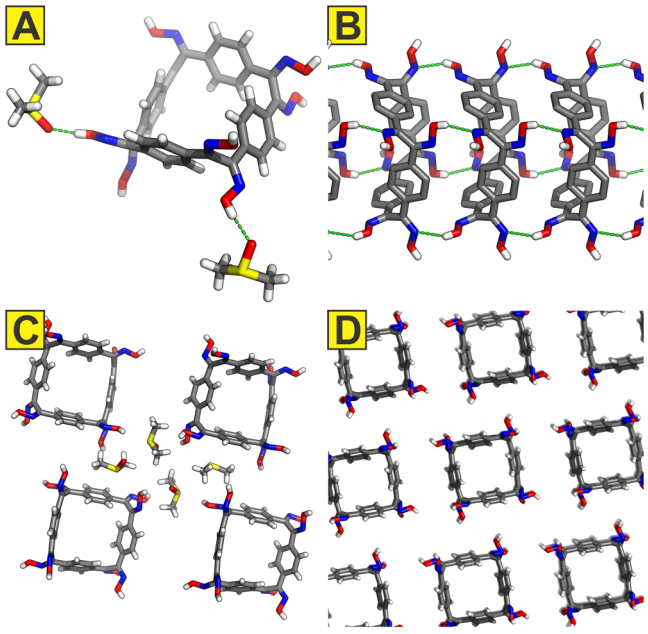

Figure 1. (A) X-ray crystal structure of oxime **2**, hydrogen bonded with two DMSO molecules. (B) Side view of a segment of a hydrogen-bonded nanotube composed of molecules of **2** (nonpolar hydrogen atoms omitted for clarity). (C) Four DMSO molecules mediate interactions between the neighboring nanotubes of **2**. (D) Overall crystal packing of **2**, shown along the crystallographic *b* axis (DMSO molecules omitted for clarity). Element colors: C—grey, O—red, N—blue, H—white, and S—yellow; hydrogen bonds are shown with green dashed lines.

bonding is observed between the oxime groups, but four of the molecule's O—H groups hydrogen bond with the solvent molecules, with [O—H···O═S] distances of 1.77 and 1.87 Å (only two interactions are shown in Figure 1A). On the other hand, molecules of **2** extensively hydrogen bond with their neighbors. Two of the oxime O—H groups pointing upward hydrogen bond with the nitrogen atoms of the neighboring molecule with [O—H···N] distances alternating between 2.17 and 2.19 Å. The two downward-pointing O—H groups establish identical hydrogen bonding pattern with another molecule of **2**, resulting in the overall organization of **2** into hydrogen-bonded nanotubes (Figure 1B). Three other notable short contacts are observed: the [C—H···O] interaction between the *ortho*-hydrogen atom of the phenylene ring and the oxime oxygen (2.62 Å), the [C—H···N] interaction between the methyl group of the DMSO molecule and the oxime nitrogen (2.59 Å), and the [C—H···S] interaction between the *ortho*-hydrogen atom of the phenylene ring and the DMSO molecule (2.95 Å). It is these last two interactions that mediate connections between the nanotubes of **2** (Figure 1C): each molecule of DMSO utilizes its methyl group to connect to one nanotube and its sulfur atom to contact the neighboring one. At the junction of four nanotubes, four DMSO molecules mediate the interactions between the nanotubes without any short contacts between the molecules of **2** from different nanotubes. The overall square-grid arrangement (Figure 1D) is thus rather like that of the parent cyclotetrabenzoin,[3] but with the notable difference that cyclotetrabenzoin nanotubes connected directly to one another through [O—H···O] hydrogen bonds between the benzoin carbonyl and hydroxy groups.

Single crystals of the oxime acetate **3** were grown over 7 days by vapor diffusion of MeCN into a solution of **2** in 1,2-dichloroethane. Acetate **3** crystallizes in $P2_1/n$ space group with two molecules per unit cell, and without included solvent. Two of the carbonyl oxygen atoms of the acetate group are disordered over two positions. The molecule also adopts a square shape, with the planes of the phenylene rings on the opposite sides of the macrocycle perfectly parallel (Figure 2A). Like in **2**, the ═N—OAc groups on the neighboring carbon atoms are pointing in the opposite directions. The inability of **3** to engage into hydrogen bonding dramatically changes its extended packing compared to that observed in **2**. Neighboring molecules of **3** establish two pairs of [C—H···O] contacts between the *ortho*-hydrogen atoms of the phenylene rings and the carbonyl oxygen atoms of the OAc group, with [C—H···O] distances of 2.48 and 2.66 Å. As the ═N—OAc groups alternate in their orientation, these contacts mediate the formation of nanotubes of molecules of **3** (Figure 2B). Each molecule of **3** is rotated by 54.5° with respect to the nanotube's running direction, in contrast to the case of **2** where each molecule's average plane was perfectly perpendicular to the nanotube's running direction. Neighboring nanotubes run in the antiparallel directions (Figure 2C), with the shortest contacts between them being the [C—H···O] interactions with distances of 2.26 and 2.37 Å. The packing diagram of **3** is shown in Figure 2D.

As the crystal structures of **2** and **3** indicated the existence of internal small voids, and their polar functional groups suggested the possibility of specific interactions, we next examined their

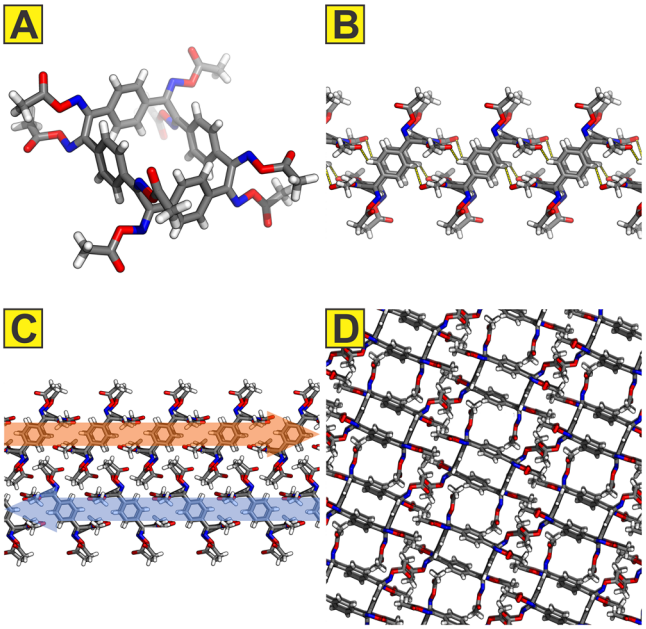

Figure 2. (A) X-ray crystal structure of oxime acetate **3**. (B) Side view of a segment of nanotubular arrangement of molecules of **3**. (C) Neighboring nanotubes run in antiparallel directions. (D) Overall crystal packing of **3**, shown along the crystallographic *b* axis. Element colors: C—grey, O—red, N—blue, and H—white; [C—H···O] short contacts shown with yellow dashed lines.

gas sorption behavior. Using CO_2 as a probe at 195 K, we determined Brunauer–Emmett–Teller (BET) surface areas of 208.8 m^2 g^{-1} for **2** and 197.2 m^2 g^{-1} for **3**. Conversely, the precursor **1** was found to be effectively nonporous with a BET surface area of 19.9 m^2 g^{-1}.[21] For compounds **2** and **3**, we therefore undertook further studies of gas sorption, focusing on CO_2, and light C_2 hydrocarbons (viz., ethane, ethylene, and acetylene), and C_3 hydrocarbons (viz., propane, propylene, and propyne). These studies were motivated by the previous observation of selective inclusion of linear guests along the central cavities of cyclobenzoin macrocycles.[22] Because of the large number of hydrogen-bonding groups in the structure of **2**, we also tested the capability of the prepared molecules for water sorption. It should be noted that powder X-ray diffraction of activated samples of **2** and **3** (but not **1**, see Figures S8–S10) indicated some loss of crystallinity.

Gas sorption isotherms for compound **2** are shown in Figure 3A–C. No hysteresis profiles were observed in the desorption cycles for N_2, CO_2, C_2, or C_3 hydrocarbon guests. Sorption isotherms for the three C_2 hydrocarbons look essentially identical, while their C_3 counterparts show the greatest volumetric sorption of propyne, followed by propene and propane. This slight preference holds even when different densities of these gases are considered (propyne—1.83 kg m^{-3}; propylene—1.91 kg m^{-3}, and propane—2.01 kg m^{-3}) in calculating molar sorption capacities. This trend is consistent with the sizes of these gas molecules and the general preference of cyclotetrabenzoin derivatives for guests with linear groups. However, the selectivity and the overall gas sorption capacity are suboptimal to render **2** a useful separation platform.

Isotherms for gas sorption in oxime acetate **3** are shown in Figure 3D–F. Under cryogenic conditions—195 K for CO_2 and 77 K for N_2—the pores of **3** were found to be accessible only to CO_2, consistent with the physicochemical properties of the two sorbates. At 195 K, CO_2 exhibits a type I isotherm, as it is near its solid–liquid transition point and readily adsorbs into micropores. In contrast, N_2 at 77 K is considerably more volatile and interacts only weakly with narrow-pore physisorbents at that temperature, leading to negligible adsorption and an apparent nonporous behavior, an observation akin to several other ultramicroporous (pore size < 7 Å) physisorbents, such as **IPM-101**,[23] **SIFSIX-dps-Cu**,[24] and **SIFSIX-23-Cu^N**.[25] Despite similar surface areas, **3** shows lower sorption of both C_2 and C_3 hydrocarbons compared to **2**. However, unlike **2**, acetate **3** shows clear discrimination between C_2 hydrocarbons, favoring the triple-bonded acetylene over ethylene and ethane. The discrimination of C_3 hydrocarbons within the pores of **3** follows the same trend already observed for **2**, but with greater apparent preference for propyne. We speculate that the more constrained apertures of pores of **3** and the strictly parallel orientation of its aromatic "walls" make its central pore better tuned for the sorption of triple-bonded guests.

Additional sorption data for the effectively nonporous **1** is shown in the Supporting Information, Figures S11,S12.

The isotherms for the sorption of water vapor in **1**–**3** are shown in Figure 4A–C, successively. While a hysteresis is noticeable in **2**, the overall adsorption capacity is slightly under 9% at 90% relative humidity, consistent with the capture of only 2–3 H_2O molecules per molecule of **2**, suggesting hydrophobic surface-driven water sorption.[26] Likewise, with clear absence of any pore filling, water sorption in octaketone **1** and acetate **3** is negligible and the hysteresis is minimal, consistent with the more hydrophobic nature of these two molecules.

3. Conclusion

We have prepared two new cyclotetrabenzil derivatives via a facile nitrogen-condensation route. Single-crystal X-ray diffraction reveals that both macrocycles assemble into nanotubular structures reminiscent of the parent cyclotetrabenzoin, albeit sustained by distinct noncovalent interactions. These findings highlight how subtle functional-group modifications can significantly influence the supramolecular assembly of shape-persistent macrocycles, and in turn affect their gas sorption selectivities. Building on these insights, ongoing studies will explore the dynamic nature of the oxime bond and strategies to stabilize individual nanotubes of **2**. The results of these investigations will be reported in due course.

Supporting Information

Synthetic procedures, crystallographic, and gas sorption analysis details.[27]

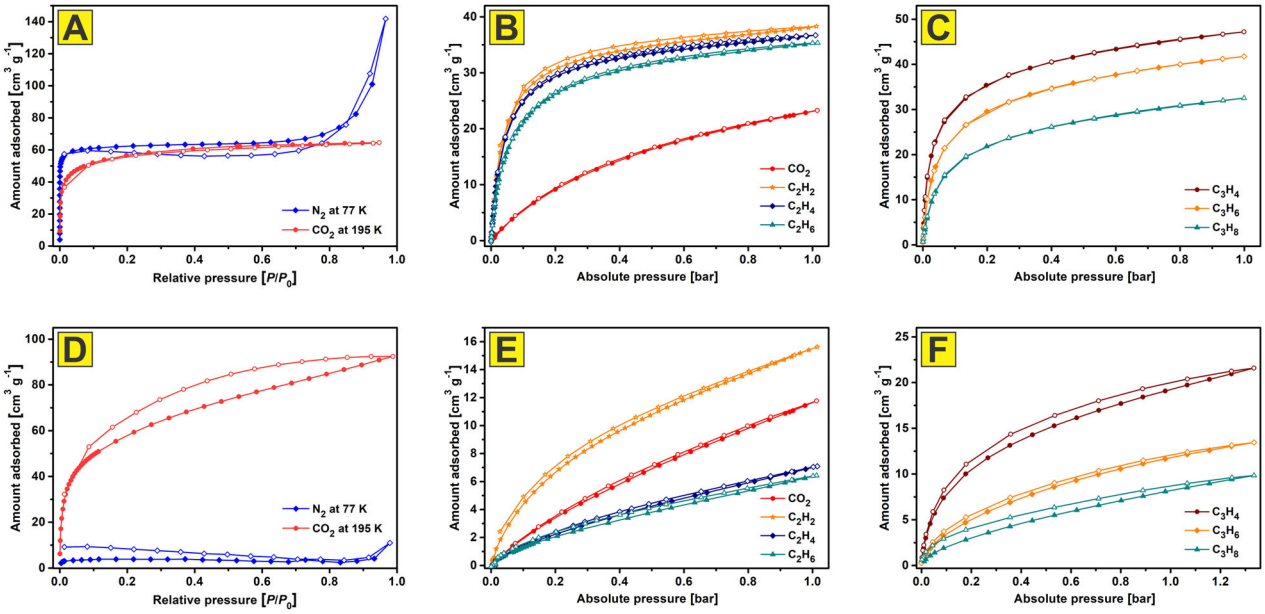

Figure 3. (A and D) N_2 (blue) and CO_2 (red) sorption isotherms for compounds **2** (A) and **3** (D). (B and E) Isotherms for the sorption of CO_2 (red) and C_2 hydrocarbons (orange—acetylene, navy—ethylene, and green—ethane) in **2** (B) and **3** (E). (C and F) Isotherms for the sorption of C_3 hydrocarbons (dark red—propyne, orange—propylene, and green—propane) in **2** (C) and **3** (F). Unless otherwise specified, all isotherms were recorded at 298 K. Closed and open symbols denote adsorption and desorption, respectively.

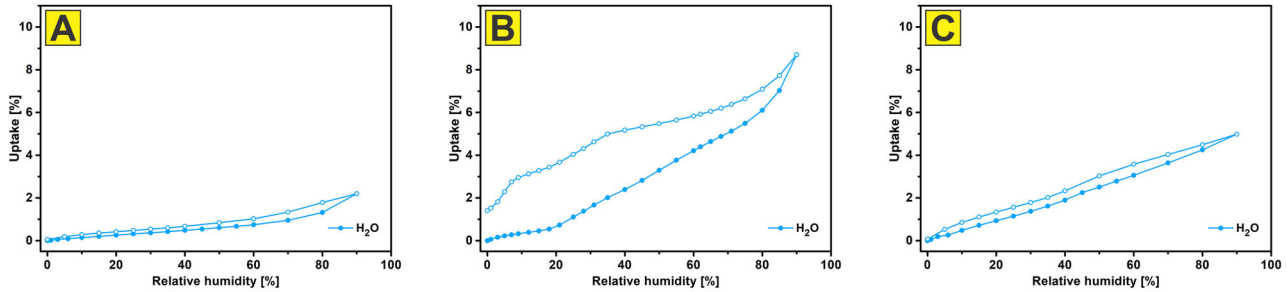

Figure 4. Water sorption isotherms for (A) octaketone **1**, (B) oxime **2**, and (**C**) its acetate **3** at 298 K. Closed and open symbols denote adsorption and desorption, respectively.

Acknowledgements

Ognjen Š. Miljanić acknowledges the generous support from the Welch Foundation (grant E-2205-20240404), the US National Science Foundation (grant CHE-2204236), and the Research Corporation for Science Advancement (2024 SEED grant). Soumya Mukherjee thanks the Research Ireland Pathway grant award 21/PATH-S/9454 and the SSPC Reward funding AzAds.

Conflict of Interests

The authors declare no conflict of interest.

Data Availability Statement

The data that support the findings of this study are available in the supplementary material of this article.

Keywords: Cyclotetrabenzoin · Gas sorption · Hydrogen bonding · Macrocycle · Oxime

[1] M. Alrayyani, O. Š. Miljanić, *Chem. Commun.* **2018**, *54*, 11989–11997.
[2] Q. Ji, L. H. Do, O. Š. Miljanić, *Synlett* **2015**, *26*, 1625–1627.
[3] Q. Ji, H. T. M. Le, X. Wang, Y.-S. Chen, T. Makarenko, A. J. Jacobson, O. Š. Miljanić, *Chem.-Eur. J.* **2015**, *21*, 17205–17209.
[4] J. Meng, A. Robles, S. Jalife, W. Ren, Y. Zhang, L. Zhao, Y. Liang, J. I. Wu, O. Š. Miljanić, Y. Yao, *Angew. Chem., Int. Ed.* **2023**, *62*, e202300892.
[5] D.-J. Yoo, M. Heeney, F. Glöcklhofer, J. W. Choi, *Nat. Commun.* **2021**, *12*, 2386.
[6] T. Ashirov, J. Lim, A. Robles, T. Puangsamlee, P. W. Fritz, A. Crochet, X. Wang, C. Hewson, P. Iacomi, O. Š. Miljanić, A. Coskun, *Angew. Chem., Int. Ed.* **2025**, *64*, e202423809.
[7] T. Ashirov, T. Puangsamlee, A. Robles, P. W. Fritz, K. Piech, O. Š. Miljanić, A. Coskun, *Helv. Chim. Acta* **2023**, *106*, e202300072.
[8] T. Ashirov, M. Alrayyani, K.-S. Song, O. Š. Miljanić, A. Coskun, *Org. Mater.* **2021**, *3*, 346–352.
[9] S. Hahn, M. Alrayyani, A. Sontheim, X. Wang, F. Rominger, O. Š. Miljanić, U. H. F. Bunz, *Chem.-Eur. J.* **2017**, *23*, 10543–10550.
[10] L. S. Xie, S. S. Park, M. J. Chmielewski, H. Liu, R. A. Kharod, L. Yang, M. G. Campbell, M. Dincă, *Angew. Chem., Int. Ed.* **2020**, *59*, 19623–19626.

[11] J. Kassa, *J. Toxicol. Clin. Toxicol.* **2002**, *40*, 803–816.
[12] L. González, J. D. Martín-Romera, P. Sánchez-Sánchez, J. A. R. Navarro, E. Barea, C. R. Maldonado, F. J. Carmona, *Inorg. Chem.* **2023**, *62*, 5049–5053.
[13] Y. Li, K. Tuo, W. Hou, C. Liang, C. Shao, Y. Sun, W. Xu, S. Cao, Y. Wang, S. Pu, Z. Li, *J. Solid State Chem.* **2025**, *346*, 125299.
[14] S. Ni, S. Chen, N. S. Alharbi, Z. Li, C. Chen, *Sep. Purif. Technol.* **2025**, *360*, 130899.
[15] Y. Qian, Y. Yuan, H. Wang, H. Liu, J. Zhang, S. Shi, Z. Guo, N. Wang, *J. Mater. Chem. A* **2018**, *6*, 24676–24685.
[16] L. Pettazzoni, M. Ximenis, F. Leonelli, G. Vozzolo, E. Bodo, F. Elizalde, H. Sardon, *Chem. Sci.* **2024**, *15*, 2359–2364.
[17] P. F. Kotikova, D. V. Dar'in, V. Yu. Kukushkin, A. Yu. Dubovtsev, *Org. Lett.* **2025**, *27*, 3465–3470.
[18] A. Y. Dubovtsev, N. V. Shcherbakov, D. V. Dar'in, V. Y. Kukushkin, *J. Org. Chem.* **2020**, *85*, 745–757.
[19] A. Kumar, V. Sridharan, *Asian J. Org. Chem.* **2021**, *10*, 1619–1637.
[20] Single crystals of **2** suitable for X-ray diffraction could be grown from a number of other solvent systems. Acetone, THF, or dioxane were used to dissolve **2** and then either hexane or pentane were diffused into the resulting solutions. While these crystals revealed a similar hydrogen bonding pattern, the presented structure was of the highest quality.
[21] Using N_2 as a probe at 77 K, we determined BET surface areas of 40.7 $m^2\ g^{-1}$ for **1** and 240.6 $m^2\ g^{-1}$ for **2**. A BET surface area for **3** could not be accurately determined.
[22] C. M. McHale, L. J. Karas, X. Wang, J. I. Wu, O. Š. Miljanić, *Org. Lett.* **2021**, *23*, 2253–2257.
[23] S. Sharma, S. Mukherjee, A. V. Desai, M. Vandichel, G. K. Dam, A. Jadhav, G. Kociok-Köhn, M. J. Zaworotko, S. K. Ghosh, *Chem. Mater.* **2021**, *33*, 5800–5808.
[24] J. Wang, Y. Zhang, P. Zhang, J. Hu, R.-B. Lin, Q. Deng, Z. Zeng, H. Xing, S. Deng, B. Chen, *J. Am. Chem. Soc.* **2020**, *142*, 9744–9751.
[25] B.-Q. Song, M. Shivanna, M.-Y. Gao, S.-Q. Wang, C.-H. Deng, Q.-Y. Yang, S. J. Nikkhah, M. Vandichel, S. Kitagawa, M. J. Zaworotko, *Angew. Chem., Int. Ed.* **2023**, *62*, e202309985.
[26] E.-P. Ng, S. Mintova, *Micropor. Mesopor. Mat.* **2008**, *114*, 1–26.
[27] Deposition Number(s) https://www.ccdc.cam.ac.uk/services/structures?id=doi:10.1002/ajoc.202500521 2445934 (for **2**) and 2445935 (for **3**) contain(s) the supplementary crystallographic data for this paper. These data are provided free of charge by the joint Cambridge Crystallographic Data Centre and Fachinformationszentrum Karlsruhe http://www.ccdc.cam.ac.uk/structuresAccess Structures service.

Manuscript received: May 1, 2025
Revised manuscript received: May 12, 2025
Version of record online: June 16, 2025